Liquid part of the phase diagram and percolation line for two-dimensional Mercedes-Benz water

T. Urbic*

Faculty of Chemistry and Chemical Technology, University of Ljubljana, Vecna Pot 113, 1000 Ljubljana, Slovenia

(Received 1 July 2017; published 15 September 2017)

Monte Carlo simulations and Wertheim's thermodynamic perturbation theory (TPT) are used to predict the phase diagram and percolation curve for the simple two-dimensional Mercedes-Benz (MB) model of water. The MB model of water is quite popular for explaining water properties, but the phase diagram has not been reported till now. In the MB model, water molecules are modeled as two-dimensional Lennard-Jones disks, with three orientation-dependent hydrogen-bonding arms, arranged as in the MB logo. The liquid part of the phase space is explored using grand canonical Monte Carlo simulations and two versions of Wertheim's TPT for associative fluids, which have been used before to predict the properties of the simple MB model. We find that the theory reproduces well the physical properties of hot water but is less successful at capturing the more structured hydrogen bonding that occurs in cold water. In addition to reporting the phase diagram and percolation curve of the model, it is shown that the improved TPT predicts the phase diagram rather well, while the standard one predicts a phase transition at lower temperatures. For the percolation line, both versions have problems predicting the correct position of the line at high temperatures.

DOI: 10.1103/PhysRevE.96.032122

I. INTRODUCTION

Water is the most important fluid in nature for life [1,2], as well as for technological processes, being one of the most important liquids in industry. Water exhibits many anomalous properties that affect life at a larger scale. Mammals rely on the high latent heat of water to cool them down through sweating. Water's high heat capacity prevents local temperature fluctuations, facilitating thermal regulation of organisms. Water has an almost-universal solvent action [3]. Nearly all known chemical substances will dissolve in water, at least to a small extent. Water is one of the most corrosive substances known and yet is physiologically harmless. In comparison to other liquids, it shows the most puzzling behavior [3,4]. The best-known examples are its density maximum at 4°C, lower density of the solid phase compared to the liquid phase, high and nearly constant heat capacity in the liquid phase negative expansion coefficient below the temperature of the density maximum, and high surface tension and viscosity. The compressibility and specific heat increase anomalously upon cooling. Water also has unusually high boiling, freezing, and critical points. These properties are largely governed by the formation of hydrogen bonds. An understanding of the hydrogen bonding (HB) is therefore crucial to understanding the behavior and properties of water and aqueous solutions. A key goal of liquid-state statistical thermodynamics is to develop quantitative theories for water and aqueous solutions (for reviews see [3–12]). A large number of models of varying complexity have been developed and analyzed to model water's extraordinary properties (for reviews, see, e.g., [13–16]), but none of the current models can correctly reproduce all the physical properties of water. In principle, the properties of water can be determined with quantum-mechanical calculations [17,18]. While they offer the highest degree of exactness, the high computational cost of these approaches limits their use to small water systems, but these insights should allow for the development and fine-tuning of simplified water models [19–21]. There have been two main approaches to modeling liquids. One approach is to perform computer simulations of atomically detailed models. These models aim for realistic detail and include variables describing van der Waals and Coulomb interactions, HB, etc. (reviewed in [10]). Such approaches can depend critically on the force field used in the calculation [22,23]. However, many properties of water and aqueous solutions can also be captured by simpler models [24,25]. One class of such simpler models has been developed by Nezbeda and coworkers [14,26,27]. One the simplest models for water is the so-called Mercedes-Benz (MB) model [28–32], which was originally proposed by Ben-Naim in 1971 [33,34]. This is a two-dimensional (2D) model. Each water molecule is modeled as a disk that interacts with other such waters through (i) a Lennard-Jones (LJ) interaction and (ii) an orientation-dependent hydrogen-bonding interaction through three radial arms arranged as in the MB logo. Interest in simplified models is due to insights that are not obtainable from all-atom computer simulations. Simpler models are more flexible in providing insights and illuminating concepts, and they do not require large computer resources. Second, simple models can explore a much broader range of conditions and external variables. Whereas simulating a detailed model may predict the behavior at a single temperature and pressure, a simpler model can be used to study a whole phase diagram of temperatures and pressures. Third, analytical models can provide functional relationships for engineering applications and lead to improved models of greater computational efficiency. Fourth, simple models can be used as a polygon to develop and study theoretical methods. Our interest in using the MB model is that it serves as one of the simplest models of an orientationally dependent liquid, so it can serve as a test bed for developing analytical theories that might ultimately be useful for more realistic models. Another advantage of the MB model, compared to more realistic water models, is that the underlying physical principles can be more readily explored and visualized in two dimensions. For the MB model, *NPT* Monte Carlo (MC) simulations have shown that the MB model

*tomaz.urbic@fkkt.uni-lj.si

predicts qualitatively the density anomaly, the minimum of the isothermal compressibility as a function of the temperature, the high heat capacity, and the experimental trends for the thermodynamic properties of solvation of nonpolar solutes [29,31,32,35] and cold denaturation of proteins [36]. The 2D MB model was also extended to three dimensions by Bizjak *et al.* [37,38] and Dias *et al.* [35,39] and studied using computer simulations [35,37–39]. The 2D model was also extensively studied with analytical methods like integral equation and thermodynamic perturbation theory [40–45]. In spite of all the MC calculations, the phase diagram and percolation curve of the model were never calculated, and that is the aim of this work: determination of the percolation line and liquid-gas coexistence line.

Even though computer simulations play an important role in understanding the properties of liquids, they can be quite time-consuming, even for simple 2D models. So it is equally important to develop simplified, more analytical approaches. For MB water, theories that have been developed for fluids comprised of molecules that associate into dimers and higher clusters can be applied. Wertheim [46–49] proposed his statistical-mechanical approach for strongly associating systems of molecules and a corresponding thermodynamic perturbation theory. In previous work [40–45,50,51], we applied Wertheim's theory to associating fluids [46,47] in the MB model and some other simple models through both a thermodynamic perturbation theory (TPT) and orientationally averaged and angle-dependent integral equation theories. We found that both the TPT and the integral equation theory approaches gave good quantitative agreement with the *NPT* MC results for the molar volume, the isothermal compressibility, and other thermodynamic properties as a function of the temperature. It is also possible to use even more analytical theories for MB-like models which allow the inclusion of orientation-dependent hydrogen bonding within a framework that is simple and nearly analytical. One such model is a statistical mechanical model, developed by Urbic and Dill [52]. The model is a direct descendant from the treatment by Truskett and Dill, who developed a nearly analytical version of the 2D MB model [53,54]. In the model each water molecule interacts with its neighboring waters through a van der Waals interaction and an orientation-dependent interaction that models hydrogen bonds. In this work, we applied the standard [40] and improved [44] TPT to calculating the phase diagram and percolation curve. Correctness of both methods was assessed by comparison with MC simulation results.

II. THE MODEL

In the MB model of water, the water molecule is represented as a 2D disk with three arms separated by a fixed angle of 120° [29,33], mimicking the formation of hydrogen bonds (Fig. 1). The water-water interaction potential between particle i and particle j is the sum of an LJ term and a hydrogen-bonding term,

$$U(\vec{X}_i,\vec{X}_j) = U_{\mathrm{LJ}}(r_{ij}) + U_{\mathrm{HB}}(\vec{X}_i,\vec{X}_j), \tag{1}$$

where r_{ij} is the distance between the center of particle i and that of particle j, and $\vec{X}_i$ is the vector representing the coordinates and orientation of the ith particle. The LJ part of the potential is determined using the standard form,

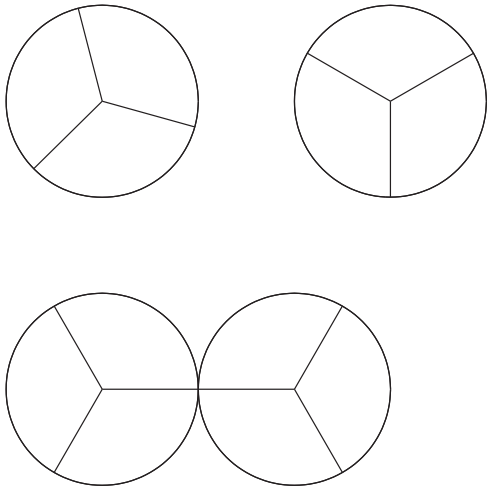

FIG. 1. MB molecules. Particles form the strongest hydrogen bond when the arms are collinear and the distance between two particles is equal to r_{HB}.

$$U_{\mathrm{LJ}}(r_{ij}) = 4\varepsilon_{\mathrm{LJ}}\left(\left(\frac{\sigma_{\mathrm{LJ}}}{r_{ij}}\right)^{12} - \left(\frac{\sigma_{\mathrm{LJ}}}{r_{ij}}\right)^{6}\right), \tag{2}$$

where $\varepsilon_{\mathrm{LJ}}$ is the depth of the LJ part of potential and σ_{LJ} is the contact value. The hydrogen-bonding part of the potential is the sum of interactions U^{kl}_{HB} between arms of different molecules:

$$U_{\mathrm{HB}}(\vec{X}_i,\vec{X}_j) = \sum_{k,l=1}^{3} U^{kl}_{\mathrm{HB}}(r_{ij},\theta_1,\theta_2). \tag{3}$$

This interaction is a Gaussian function in distance and both angles,

$$U^{kl}_{\mathrm{HB}}(r_{ij},\theta_1,\theta_2) = \varepsilon_{\mathrm{HB}}G(r_{ij}-r_{\mathrm{HB}})G(\vec{i}_k\vec{u}_{ij}-1)G(\vec{j}_l\vec{u}_{ij}+1) \tag{4}$$

$$\begin{aligned} &= \varepsilon_{\mathrm{HB}}G(r_{ij}-r_{\mathrm{HB}}) \\ &\quad\times G\left(\cos\left(\theta_i+\frac{2\pi}{3}(k-1)\right)-1\right) \\ &\quad\times G\left(\cos\left(\theta_j+\frac{2\pi}{3}(l-1)\right)+1\right). \end{aligned} \tag{5}$$

$\varepsilon_{\mathrm{HB}} = -1$ is an HB energy parameter and $r_{\mathrm{HB}} = 1$ is a characteristic HB length. $\vec{u_{ij}}$ is the unit vector along $\vec{r_{ij}}$ and $\vec{i_k}$ is the unit vector representing the kth arm of the ith particle, where θ_i is the orientation of the ith particle and $G(x)$ is an unnormalized Gaussian function,

$$G(x) = \exp\left(-\frac{x^2}{2\sigma^2}\right). \tag{6}$$

The strongest hydrogen bond occurs when an arm of one particle is colinear with the arm of another particle and the two arms point in opposing directions. The LJ well depth $\varepsilon_{\mathrm{LJ}}$ is 0.1 times the HB interaction energy $\varepsilon_{\mathrm{HB}}$ and the Lennard-Jones contact parameter σ_{LJ} is $0.7r_{\mathrm{HB}}$. The width of the Gaussian for

distances and angles ($\sigma = 0.085 r_{HB}$) is small enough that a direct hydrogen bond is more favorable than a bifurcated one.

III. MONTE CARLO COMPUTER SIMULATION

To calculate the phase diagram and study the percolation properties, we performed MC simulations in the grand canonical ensemble (constant μ, V, and T) [55]. Periodic boundary conditions and the minimum image convention were used to mimic an infinite system of particles. Starting configurations were selected randomly. In each move, we randomly tried to translate or rotate random particles or to insert or remove random particles. Probabilities for translation, rotation, and exchange of particles were the same. In one cycle, we tried to translate and rotate each particle on average and to make as many insertions and removals as the average number of particles in the system. The simulations were allowed to equilibrate for 50 000 cycles and averages were taken for 20 series, each consisting of another 50 000 cycles, to obtain well-converged results. In the system we had from 50 to 500 particles, depending on the density of the system. Note that 100 molecules in two dimensions is equivalent to 1000 particles in three dimensions. Thermodynamic quantities such as the energy were calculated as statistical averages over the course of the simulations [55]. The cutoff of the potential was the half-length of the simulation box. Increasing the number of particles had no significant effect on the calculated quantities. In addition to the MB water simulations described above, we also performed simulations in the canonical (NVT) ensemble [55]. One purpose of this calculation was to calculate the pressure by means of the virial equation [55] and to perform the cluster analysis, which is used to classified the overall bonding state of the system. The cluster and bond analyses use an energy criterion wherein water molecules are considered bonded when their hydrogen-bonded energy is less than -0.05. Small variations in this energy cutoff did not account for significant differences in the bonding state of the system. The percolation line was determined as the density at which at least 50% of water particles were part of one big cluster connected by hydrogen bonds.

IV. THERMODYNAMIC PERTURBATION THEORY

Here is a brief overview of Wertheim's first-order perturbation theory [46,56], used previously [40,41,44]. The Helmholtz free energy for MB molecules is the sum of an ideal term, A_{id}, a reference term, A_{LJ}, and a perturbation term, A_{HB}. The latter takes into account the association of MB molecules into hydrogen-bonded networks,

$$\frac{A}{Nk_BT} = \frac{A_{id}}{Nk_BT} + \frac{A_{LJ}}{Nk_BT} + \frac{A_{HB}}{Nk_BT}, \tag{7}$$

where N is the number of particles, T is the temperature, and k_B is Boltzmann's constant. The term A_{LJ} was determined using the Barker-Henderson perturbation theory [40,57]. The use of other perturbation methods for the Lennard-Jones part did not improve the results. In Barker-Henderson theory, the reference system was the hard-disk system

$$\frac{A_{LJ}}{Nk_BT} = \frac{A_{HD}}{Nk_BT} + \frac{\rho}{2k_BT}\int_{\sigma_{LJ}}^{\infty} g_{HD}(r,\eta)u_{LJ}(r)d\vec{r}, \tag{8}$$

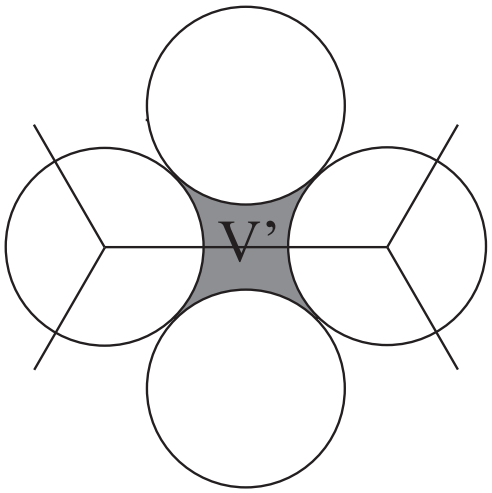

FIG. 2. Definition of the excluded volume in the modified version of the TPT.

where A_{HD} is the hard-disk part of the Helmholtz free energy, ρ is the number density of water particles, η is the packing fraction of the hard-disk reference system, and $g_{HD}(r,\eta)$ is the pair distribution function of the hard-disk reference fluid [40]. We calculated the contribution of hydrogen bonding to the Helmholtz free energy using

$$\frac{A_{HB}}{Nk_BT} = 3\left(\log x - \frac{x}{2} + \frac{1}{2}\right), \tag{9}$$

where x is the fraction of molecules not bonded at one particular arm. x is obtained from the mass-action law [46] in the form

$$x = \frac{1}{1 + 3\rho x \Delta}. \tag{10}$$

Finally, Δ is defined by [46,56]

$$\Delta = 2\pi \int g_{LJ}(r,\rho)\bar{f}_{HB}(r)rdr, \tag{11}$$

where $\bar{f}_{HB}(r)$ is an orientationally averaged Mayer function for the hydrogen-bonding potential of one site. The pair distribution function $g_{LJ}(r)$ is obtained by solving the Percus-Yevick equation for Lennard-Jones disks. Once the Helmholtz free energy is known, other thermodynamic quantities may be calculated using standard thermodynamic relations [57].

The difference between the improved TPT [44] and the standard TPT is that, instead of the density ρ, we use the effective density ρ^{ef} in Eqs. (7)–(11) as an effective density, which is calculated as explained below. The logic for this is that the particles cannot access the whole space in the system when they form bonds. When two water molecules form a hydrogen bond, it sterically occludes space, which becomes inaccessible to any other molecule (see Fig. 2). The effective particle volume was calculated as

$$V^{ef} = \frac{1}{\rho} - \frac{\bar{n}V'}{2}, \tag{12}$$

where V' is the volume not accessible to other molecules when two molecules form a hydrogen bond and can be

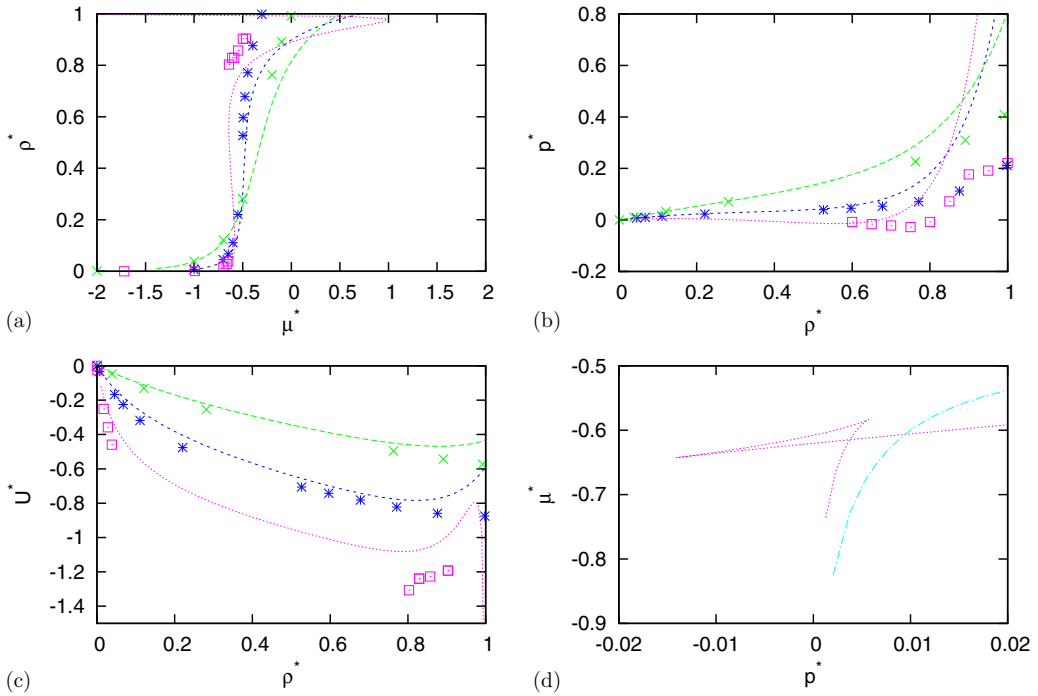

FIG. 3. (a) Density as a function of chemical potential for different temperatures. The jump indicates a liquid-gas phase transition. (b) Pressure as a function of density for different temperatures. Below the critical point, we can see nonmonotonic behavior of the pressure, and with Maxwell construction, the coexistence line can be calculated. (c) Internal energy as a function of density for different temperatures. In (a)–(c) results from computer simulations are plotted with symbols; results from the improved TPT, with lines. (d) An alternative to Maxwell construction is to plot the chemical potential as a function of the pressure in the region of phase transition. Results were calculated by the improved TPT method for different temperatures. The intersection of the curve is where there is coexistence of phases. Green symbols, high temperature, $T^* = 0.3$; blue symbols, $T^* = 0.2$; and pink symbols, low temperature, $T^* = 0.15$.

approximated by simple geometry. Two water molecules that form a hydrogen bond are separated by a distance 1. If the LJ core is approximated by the diameter d of HD molecules from Barker-Henderson perturbation theory, V' can be approximated as

$$V' = \sqrt{d^2 - \frac{1}{2}} - \frac{\pi d^2}{4}. \tag{13}$$

In Eq. (12), $\bar{n}$ is the average number of hydrogen bonds per molecule. Each molecule has three arms. The probability that a hydrogen bond is formed at one arm is $(1 - x)$, where x is the ratio of nonbonded molecules at one arm. We now get

$$\bar{n} = 3(1 - x). \tag{14}$$

The effective particle density can now be calculated as

$$\rho^{\mathrm{ef}} = \frac{1}{V^{\mathrm{ef}}}. \tag{15}$$

Now, the set of Eqs. (10)–(15) must be solved iteratively to get the effective density, ρ^{ef}, and the fraction of molecules x that are not hydrogen bonded. The effective packing fraction is then calculated as $\eta^{\mathrm{ef}} = \rho^{\mathrm{ef}} \pi d^2/4$. Once the effective density and packing fraction are known, the Helmholtz free energy can be calculated with Eqs. (7)–(9), and other thermodynamic properties with standard thermodynamic relations [57].

V. RESULTS AND DISCUSSION

All our results reported below are given in reduced units; the excess internal energy and temperature are normalized to the HB energy parameter $\varepsilon_{\mathrm{HB}}(A^* = \frac{A}{|\varepsilon_{\mathrm{HB}}|}, T^* = \frac{k_B * T}{|\varepsilon_{\mathrm{HB}}|})$ and the distances are scaled to the hydrogen-bond characteristic length $r_{\mathrm{HB}}(r^* = \frac{r}{r_{\mathrm{HB}}})$. Errors in MC simulations are the size of the symbols used to present the data.

In the first step, we determined the gas-liquid part of the phase diagram for the MB model of water by computer simulation. We did this by performing MC simulations in the grand canonical ensemble. We calculated the dependence of the density as a function of the chemical potential at a constant temperature. Results for selected temperatures are plotted in Fig. 3(a) as symbols. For temperatures above the critical point the function is smooth, while for temperatures below we observe a jump in density between the gas and the liquid densities, which are in coexistence. In Fig. 3(a) we also plot results from the improved TPT. For the high temperature, $T^* = 0.3$ (green line and symbols), the TPT reproduces the MC data very well for densities up to 1. At the midrange temperature $T^* = 0.2$ (blue line and symbols) we can observe a similar agreement, while at the cold temperature $T^* = 0.15$ (pink line and symbols) the improved TPT shows phase transition behavior. At all temperatures there is disagreement between TPT and MC results at high densities, where the improved TPT starts to fail. In the improved and standard TPT, we can determine gas and liquid phases which coexist by doing a Maxwell construction for the chemical potential as a function

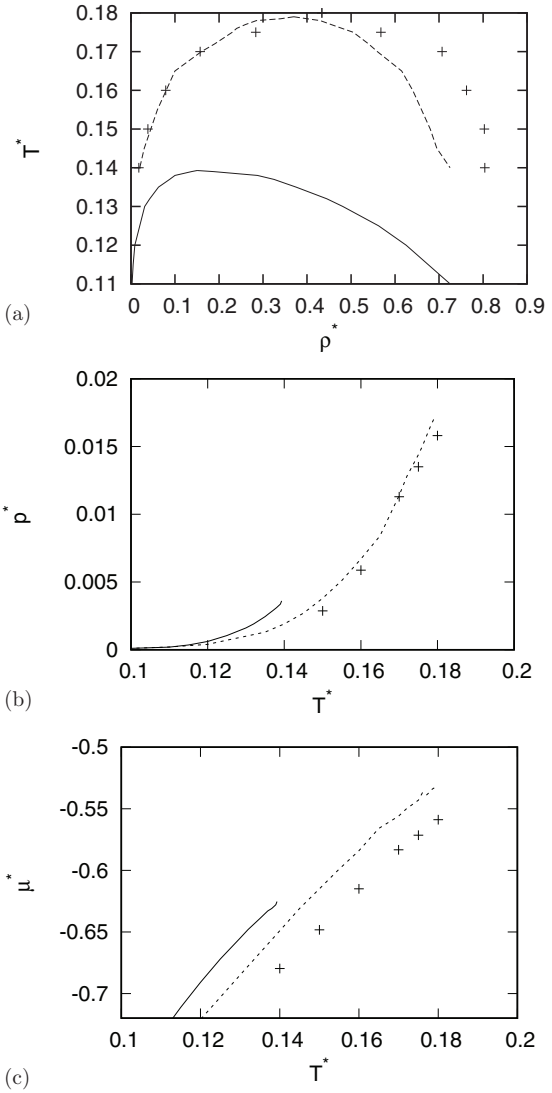

FIG. 4. Vapor-liquid equilibria from MC and TPT. Results from computer simulations are plotted as symbols; results from the TPT, as a solid line; and results from the improved TPT, as a dotted line. (a) T^*-ρ^* liquid-gas coexistence; (b) T^*-p^* coexistence; and (c) T^*-μ^* coexistence.

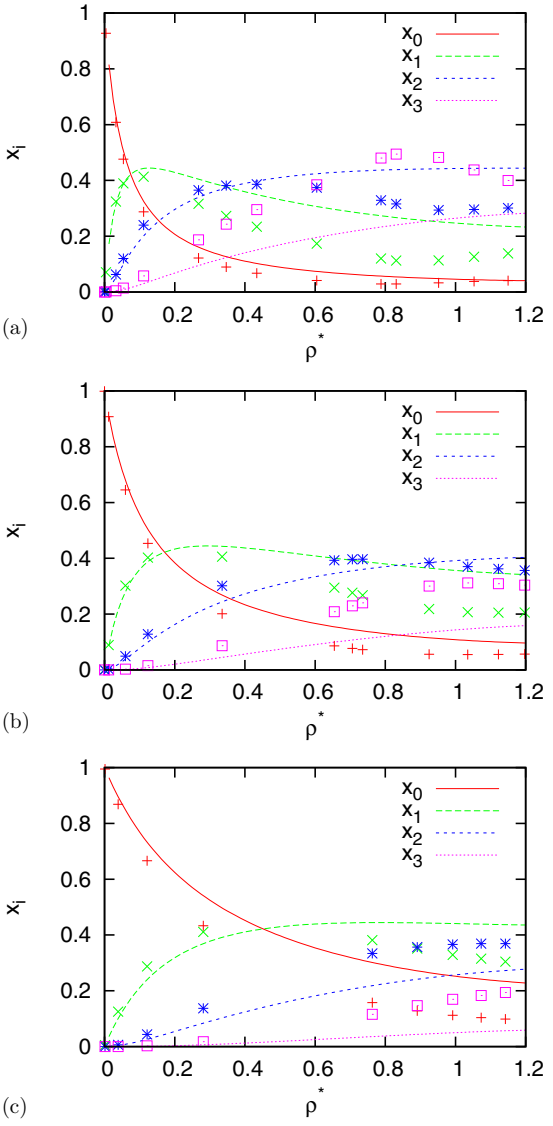

FIG. 5. Density dependence of ratios of molecules with zero, one, two, and three hydrogen bonds. Symbols are the results from Monte Carlo computer simulations; lines, from the standard TPT. Results are plotted for different temperatures: (a) $T^* = 0.18$, (b) $T^* = 0.22$, and (c) $T^* = 0.3$.

of the volume (inverse density). Another way to determine this is by plotting the pressure as a function of the density, which is done in Fig. 3(b) for different temperatures. In MC simulations, the pressure was calculated using a virial route in the *NVT* ensemble. The agreement between the improved TPT and the MC data is similar to that observed for the chemical potential. Also, here we can do Maxwell construction to determine the liquid-gas coexistence densities. To further test the improved TPT, we checked how good TPT is at reproducing the internal energy U^*. The comparison is plotted in Fig. 3(c). We can see that the agreement is quantitative; TPT can predict correct trends but cannot predict correct values exactly. An alternative to doing Maxwell construction to determine the gas-liquid coexistence densities for both versions of the TPT is by plotting the chemical potential as a function of the pressure. The curve in the region below the critical point intersects at the coexistence pressure, as demonstrated in Fig. 3(d) (the temperature below the critical temperature has an intersection, while the curve above does not). Doing these calculations for both versions of the TPT and for the MC simulations, we were able to determine the gas-liquid coexistence lines, which are plotted in Fig. 4. This figure shows a comparison of the gas-liquid equilibrium curves calculated by MC and both TPT methods. The critical point for the gas-liquid transition obtained by MC is $T_c^* = 0.18$, $p_c^* = 0.016 \mu_c^* = -0.56$, and $\rho_c^* = 0.433$; that by standard TPT is $T_c^* = 0.14$, $p_c^* = 0.0036$, $\mu_c^* = -0.625$, and $\rho_c^* = 0.150$; and that by improved TPT is $T_c^* = 0.179$, $p_c^* = 0.017$, $\mu_c^* = -0.533$, and $\rho_c^* = 0.370$. We can see that the improved TPT predicts the correct critical point rather well, while the standard TPT predicts it at a lower temperature, density, and pressure. The reasons include the position of the arms, which are not on the surface of the LJ disk but farther away from the surface. Thus there

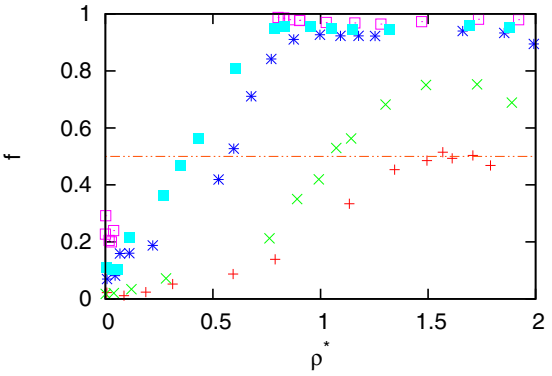

FIG. 6. Fraction of molecules belonging to the biggest cluster as a function of the density for different temperatures. Symbol are the results from Monte Carlo computer simulations. Red symbols, high temperature, $T^* = 0.4$; green symbols, $T^* = 0.3$; blue symbols, $T^* = 0.2$; light-blue symbols, low temperature, $T^* = 0.18$; and pink symbols, low temperature, $T^* = 0.15$.

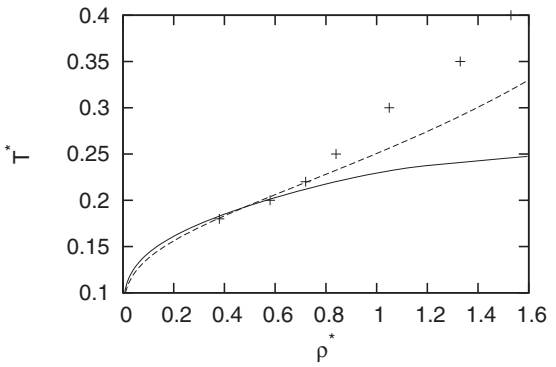

FIG. 7. Percolation line from MC and TPT. Results from computer simulations are plotted with symbols; results from the TPT, with the solid line; and results from the improved TPT, with the dashed line.

is a part of the space inaccessible to molecules which is corrected in the improved TPT. We also checked the possibility of a liquid-liquid phase transition of the model, but due to crystallization issues we cannot calculate this with the current version of the MC method, and both TPT methods fail to detect any liquid-liquid phase transition.

We continued our study toward determining the percolation line, first by calculating the ratios of molecules with zero, one, two, and three hydrogen bonds. In the MC simulation, we analyze the average number of water molecules forming zero, one, two, and three hydrogen bonds during the MC run. In TPT, we calculate this from the fraction of molecules not bonded at one particular arm x as $x_0 = x^3$, $x_1 = 3x^2(1-x)$, $x_2 = 3x(1-x)^2$, and $x_3 = (1-x)^3$. Results for different temperatures are presented in Fig. 5. TPT results are presented for the standard version of TPT. Predictions for the fraction are semiaccurate. Surprisingly, the agreement for the ratio of molecules with no hydrogen bonds is worst for higher temperatures. TPT does quite well for one and two bonded molecules at all temperatures and densities. The worst agreement is for molecules with three hydrogen bonds, where we have bad agreement at all temperatures and densities. Next we checked how the system is connected by hydrogen bonds. We performed cluster analysis and checked the fraction of water molecules belonging to the biggest cluster in the system by MC computer simulations. Results are plotted in Fig. 6. At a constant temperature, the fraction of molecules belonging to the biggest cluster connected by hydrogen bonds increases with the density, reaches a maximum, and then, due to high packing, starts to decrease. This happens at densities higher than that of the perfect hexagonal crystal. In MC, the percolation line was determined as the density at which at least 50% of water particles were part of one big cluster connected by hydrogen bonds. In TPT, we followed Bianchi *et al.* [58], where the ratio of nonbonded particles at a particular arm at percolation x_p is equal to 0.5. Percolation curves determined with these methods are presented in Fig. 7 for MC simulations and both versions of the TPT. We can see that since the calculation in TPT is based on ratios of free particles, and since the agreement with MC is not good at high temperatures, the TPT curves deviate from the MC results in that region. The TPT predicts a connected system at lower temperatures than the MC does.

VI. CONCLUSIONS

Monte Carlo simulations and Wertheim's thermodynamic perturbation theory (TPT) are used to predict the phase diagram and percolation curve of the simple Mercedes-Benz (MB) model of water. The MB model balances Lennard-Jones interactions with an orientation dependence that is intended to mimic hydrogen bonding. The MB model has previously been shown to have the volume anomalies of pure water and the thermal anomalies of nonpolar solvation. The TPT method is orders of magnitude more efficient than the Monte Carlo simulations. We have determined the liquid-gas part of the phase diagram and percolation curve and pinpointed the area where there is gas-liquid coexistence and the phase space where the system is connected by hydrogen bonds. For the MB model of water, we did not observe any liquid-liquid phase transition in the area of observation by Monte Carlo or TPT. If it exists, it is present in the supercooled region, but in the Monte Carlo this is difficult to study due to crystallization. We find that the improved TPT method reproduces well the physical properties of water in the area of the phase transition investigated, while the standard TPT predicts coexistence at lower temperatures. Both theories are able to predict the percolation line at lower temperatures but fail to predict it at high temperatures. The TPT methods show an error in the prediction of the ratio of nonbonded particles at one arm. This error is magnified at higher temperatures when calculating the percolation curve.

ACKNOWLEDGMENTS

This work was supported by the NIH (Grant No. GM063592), the Slovenian Research Agency (Grants No. P1 0103-0201 and No. N1-0042), and the National Research, Development and Innovation Office of Hungary (Grant No. SNN 116198).

[1] M. Chaplin, Nat. Rev. Mol. Cell Biol. **7**, 861 (2006).
[2] M. J. Tait and F. Franks, Nature **230**, 91 (1971).
[3] Edited by F. Franks, *Water, a Comprehensive Treatise*, *Vols. 1–7* (Plenum Press, New York, 1972–1980).
[4] D. Eisenberg and W. Kauzmann, *The Structure and Properties of Water* (Oxford University Press, Oxford, UK, 1969).
[5] F. H. Stillinger, Science **209**, 451 (1980).
[6] C. Tanford, *The Hydrophobic Effect: Formation of Micelles and Biological Membranes*, 2nd ed. (Wiley, New York, 1980).
[7] W. Blokzijl and J. B. F. N. Engberts, Angew. Chem., Int. Ed. Engl. **32**, 1545 (1993).
[8] G. Robinson, S.-B. Zhu, S. Singh, and M. Evans, *Water in Biology, Chemistry and Physics: Experimental Overviews and Computational Methodologies* (World Scientific, Singapore, 1996).
[9] R. Schmidt, Monatsh. Chem. **132**, 1295 (1993).
[10] B. Guillot, J. Mol. Liq. **101**, 219 (2002).
[11] A. Ben-Naim, Biophys. Chem. **105**, 183 (2003).
[12] L. R. Pratt, Annu. Rev. Phys. Chem. **53**, 409 (2002).
[13] W. L. Jorgensen, J. Chandrasekhar, J. D. Madura, R. W. Impey, and M. L. Klein, J. Chem. Phys. **79**, 926 (1983).
[14] I. Nezbeda, J. Mol. Liq. **73-74**, 317 (1997).
[15] P. Gallo, K. Amann-Winkel, C. A. Angell, M. A. Anisimov, F. Caupin, C. Chakravarty, E. Lascaris, T. Loerting, A. Z. Panagiotopoulos, J. Russo, J. A. Sellberg, H. E. Stanley, H. Tanaka, C. Vega, L. Xu, and L. G. M. Pettersson, Chem. Rev. **116**, 7463 (2016).
[16] C. Vega, J. L. F. Abascal, M. M. Conde, and J. L. Aragones, Faraday Discuss. **141**, 251 (2009).
[17] K. B. Lipkowitz, D. B. Boyd, S. J. Smith, and B. T. Sutcliffe, Rev. Comput. Chem. **10**, 271 (2007).
[18] E. J. Baerends and O. V. Gritsenko, J. Phys. Chem. A **101**, 5383 (1997).
[19] D. van der Spoel, P. J. van Maaren, and H. J. C. Berendsen, J. Chem. Phys. **108**, 10220 (1998).
[20] H. W. Horn, W. C. Swope, J. W. Pitera, J. D. Madura, T. J. Dick, G. L. Hura, and T. Head-Gordon, J. Chem. Phys. **120**, 9665 (2004).
[21] J. L. F. Abascal and C. Vega, J. Chem. Phys. **123**, 234505 (2005).
[22] J-C. Soetens, C. Millot, C. Chipot, G. Jansen, J. G. Angyán, and B. Maigret, J. Phys. Chem. B **101**, 10910 (1997).
[23] B. Hess and Nico F. A. van der Vegt, J. Phys. Chem. B **110**, 17616 (2006).
[24] T. M. Truskett, P. G. Debenedetti, S. Sastry, and S. Torquato, J. Chem. Phys. **111**, 2647 (1999).
[25] K. A. Dill, T. M. Truskett, V. Vlachy, and B. Hribar-Lee, Annu. Rev. Biophys. Biomol. Struct. **34**, 173 (2005).
[26] I. Nezbeda, J. Kolafa, and Yu. V. Kalyuzhnyi, Mol. Phys. **68**, 143 (1989).
[27] I. Nezbeda and G. A. Iglezias-Silva, Mol. Phys. **69**, 767 (1990).
[28] G. Andaloro and R. M. Sperandeo-Mineo, Eur. J. Phys. **11**, 275 (1990).
[29] K. A. T. Silverstein, A. D. J. Haymet, and K. A. Dill, J. Am. Chem. Soc. **120**, 3166 (1998).
[30] K. A. T. Silverstein, K. A. Dill, and A. D. J. Haymet, Fluid Phase Equil. **120**, 3166 (1998).
[31] N. T. Southall and K. A. Dill, J. Phys. Chem. B **104**, 1326 (2000).
[32] K. A. T. Silverstein, K. A. Dill, and A. D. J. Haymet, J. Chem. Phys. **114**, 6303 (2001).
[33] A. Ben-Naim, J. Chem. Phys. **54**, 3682 (1971).
[34] A. Ben-Naim, Mol. Phys. **24**, 705 (1972).
[35] C. L. Dias, T. Hynninen, T. Ala-Nissila, A. S. Foster, and M. Karttunen, J. Chem. Phys. **134**, 065106 (2011).
[36] C. L. Dias, Phys. Rev. Lett. **109**, 048104 (2012).
[37] A. Bizjak, T. Urbic, V. Vlachy, and K. A. Dill, Acta Chim. Slov. **54**, 532 (2007).
[38] A. Bizjak, T. Urbic, V. Vlachy, and K. A. Dill, J. Chem. Phys. **131**, 194504 (2009).
[39] C. L. Dias, T. Ala-Nissila, M. Grant, and M. Karttunen, J. Chem. Phys. **131**, 054505 (2009).
[40] T. Urbic, V. Vlachy, Yu. V. Kalyuzhnyi, N. T. Southall, and K. A. Dill, J. Chem. Phys. **112**, 2843 (2000).
[41] T. Urbic, V. Vlachy, Yu. V. Kalyuzhnyi, N. T. Southall, and K. A. Dill, J. Chem. Phys. **116**, 723 (2002).
[42] T. Urbic, V. Vlachy, Yu. V. Kalyuzhnyi, and K. A. Dill, J. Chem. Phys. **118**, 5516 (2003).
[43] T. Urbic, V. Vlachy, O. Pizio, and K. A. Dill, J. Mol. Liq. **112**, 71 (2004).
[44] T. Urbic, V. Vlachy, Yu. V. Kalyuzhnyi, and K. A. Dill, J. Chem. Phys. **127**, 174511 (2007).
[45] T. Urbic and M. F. Holovko, J. Chem. Phys. **135**, 134706 (2011).
[46] M. S. Wertheim, J. Stat. Phys. **42**, 477 (1986).
[47] M. S. Wertheim, J. Chem. Phys. **87**, 7323 (1987).
[48] M. S. Wertheim, J. Chem. Phys. **88**, 1145 (1987).
[49] M. S. Wertheim, J. Chem. Phys. **85**, 2929 (1986).
[50] T. Urbic, J. Mol. Liq. **228**, 32 (2017).
[51] T. Urbic, J. Mol. Liq. **238**, 129 (2017).
[52] T. Urbic and K. A. Dill, J. Chem. Phys. **132**, 224507 (2010).
[53] T. M. Truskett and K. A. Dill, J. Chem. Phys. **117**, 5101 (2002).
[54] T. M. Truskett and K. A. Dill, J. Phys. Chem. B **106**, 11829 (2002).
[55] D. Frenkel and B. Smit, *Molecular Simulation: From Algorithms to Applications* (Academic Press, New York, 2000).
[56] G. Jackson, W. G. Chapman, and K. E. Gubbins, Mol. Phys. **65**, 1 (1988).
[57] J. P. Hansen and I. R. McDonald, *Theory of Simple Liquids* (Academic Press, London, 1986).
[58] E. Bianchi, P. Tartaglia, E. Zaccarelli, and F. Sciortino, J. Chem. Phys. **128**, 144504 (2008).